



Comparative study of floor response spectra for regular and irregular buildings subjected to earthquake

M. V. Landge¹ · R. K. Ingle¹

Received: 5 February 2020 / Accepted: 3 August 2020 / Published online: 9 August 2020
© Springer Nature Switzerland AG 2020

Abstract

Past earthquakes have resulted in structural collapse and failure of non-structural components. In the nuclear, chemical, and hazardous industry, working on no-failure conditions of non-structural components after an earthquake is sensible. It has been observed that to minimize financial loss and to avoid fears of life safety, non-structural components should be designed for proper seismic forces. This design has been based on a maximum inertia force, which is interrelated to the floor response spectra. Therefore, the primary objective of the current study is to recognize and quantify the acceleration floor amplification of the low-rise building models. This paper aims to obtain the elastic and inelastic acceleration response of regular building and buildings having irregularity such as mass and stiffness irregularity located at the lower and higher storey, and vertical geometric irregular buildings. It perceived that input ground motion characteristics govern the response of lower storey. Also, floor response spectra are indicating distinct peaks analogous to contributing modes due to the dynamic characteristics of the building. Due to the dynamic filtering effect, the floor accelerogram intensified concerning the base and has an enormous frequency content for the periods, near to the modal time periods of the elastic model.

Keywords Acceleration time history · Floor response spectra · Non-structural components · Mass and stiffness irregularity · Vertical geometric irregularity · Peak floor spectral acceleration · Peak ground acceleration

Introduction

Past earthquakes such as 1906 San Francisco, 1925 Santa Barbara, 1933 Long Beach, 1952 Bakersfield, 1964 Alaska, 1971 San Fernando, 1987 Whittier-Narrows, 1989 Loma Prieta, 1994 Northridge, and 2001 Bhuj have resulted in structural collapse and failure of non-structural components (NSCs). In the nuclear, chemical, and hazardous industry, working on no-failure conditions of non-structural components (NSCs) such as generators, condensers, and several much more critical equipment's involving control systems, mechanical systems, and electrical systems after an earthquake are sensible. NSCs support generally attached to the floors or walls of primary systems. When an earthquake occurs, support suffered due to the vibration of the floor to which they have connected. To design supports for these NSCs, an acceleration history at every floor in the building

has developed for the maximum admirable earthquake. These floor acceleration time histories are an amplification of the acceleration time history of the ground during an earthquake, based on the stiffness and mass configuration of the building.

A usual method for designing NSCs includes the usage of Floor Response Spectra (FRS). The FRS method is a decoupled analysis method (Suarez and Singh 1987; Adam 2001; Kumar et al. 2011; Menon and Magenes 2011; Surana et al. 2018) in which the primary and secondary systems assessed independently. A dynamic analysis is done first for the primary structure, neglecting the consideration of the effect of the secondary system. The input for the analysis of fundamental structures is compatible time histories with recommended ground motion history. Responses of the primary structure, as acceleration history of the floor at the locations of the secondary systems, is considered as the input to a single-degree-of-freedom system to generate floor response spectra. Thus, the maximum response for the design of the secondary system supports estimated using the generated FRS. The initial study of the response of NSCs was in concern with the protection of critical components in nuclear

✉ M. V. Landge
mjdvnit2015@gmail.com

¹ Department of Applied Mechanics, VNIT, Nagpur 440010, India

power plants by Biggs and Roesset (1970) which further directed to the development of the US Nuclear Regulatory Guide (1978). Biggs and Roesset (1970), Amin et al. (1971), and Singh and Ang (1974) used the ground acceleration spectrum for deriving the floor acceleration spectrum. But due to long numerical integrations method was impractical (Villaverde 1997). The state of the art article on NSCs was dealt with in more detail (Chen and Soong 1988; Soong 1994; Villaverde 2004), and they recognized the key restriction of the earlier methods based on the assumption that the NSC and supporting primary structure respond in the elastic range. However, for the supporting structure, the inelastic behavior shows a substantial reduction in floor accelerations (Lin and Mahin 1985). Analogous interpretations also were demonstrated by Rodriguez et al. (2002), Chaudhuri and Villaverde (2008), Weiser et al. (2013), and Flores et al. (2015).

Agrawal and Datta (2003) reported that the yielding of the primary system impacts the response of the secondary system in a complicated way. Medina et al. (2006) point out that the shape and magnitude of FRS for light components placed on primary frame structures sensitively influenced by the modal periods, the strength of the supporting structure and the location of NSCs. Singh et al. (2006a, b) detected noteworthy variances in the recorded acceleration values with code provisions due to building's irregularity, higher modes, and ground motion characteristics.

The most significant manipulating factors for FRS are period of building, damping of the component and the inelasticity experienced by the primary structure suggested by the Sankaranarayanan and Medina (2007). They also projected acceleration response modification factor to increase and decrease in FRS value due to yielding of the primary structure. Shooshtari et al. (2010) observed that building with a short period showed a significantly amplified floor response. The ratio between Peak Floor Acceleration (PFA) and Peak Ground Acceleration (PGA) increases the ground acceleration spectrum to accomplish anticipated floor acceleration spectrum using special moment resisting frame analysed by Wieser et al. (2013). A comparison between the elastic and inelastic FRS carried out by Petrone et al. (2015) represents a significant decrease in peak spectral ordinate accompanying the first mode. To minimize financial loss and to avoid fears of life safety, NSCs must be designed for proper seismic forces. This design based on a maximum inertia force, which is interrelated to the FRS. Research work related to this is in progress but less focused on the effect of different building irregularities on FRS. Therefore, the primary objective of this study is to recognize and quantify the acceleration floor amplification of the low-rise building models, which is the most significant parameter impacting the design of NSCs. This paper aims to obtain the elastic and inelastic acceleration response of regular building and buildings having irregularity such as mass and stiffness

irregularity located at the lower and higher storey, and vertical geometric irregular buildings.

Buildings designated for analysis

5-storey reinforced concrete, 2D moment-resisting bare frame buildings, one regular (M_0), and remaining with different types of irregularities such as mass irregular ($M_1; M_2$), stiffness irregular ($M_3; M_4$), and vertical geometric irregular ($M_5; M_6; M_7; M_8; M_9$), buildings as shown in Fig. 1, has been considered. In model M_1 and M_2 , the seismic weight of the first floor and fifth floor, respectively, taken as 200%, than that of the adjacent floor levels. In model M_3 and M_4 , the storey height of the first and fifth floors, respectively, taken as 1.5 times than that of the adjoining floor levels. In M_5, M_6, M_7, M_8, M_9 , the horizontal dimension (L_2) of the lateral load resisting system is higher than the 125% of the storey above (L_1). L_2 and L_1 shown in Fig. 1 and its ratio shown in Table 1. Thus, all irregular building frames satisfying irregularity criteria as per IS 1893 (Part 1) (2016).

According to building types of HAZUS (2006), recognized buildings represent a low-rise building. The bare frame considered as a special moment-resisting frame (SMRF). The building has situated on medium soil and located in the highest seismic zone. A constant 4 m bay width and 3 m storey height are taken for all frames and all floors. The reinforced concrete (RC) has modeled with M30 grade (nominal characteristic compressive strength of 30 MPa) and the reinforcing steel with HYSD 415 (characteristic yield strength of 415 MPa). Unit weight of RC has taken as 25 kN/m³ as per IS 875-Part 1 (1987), and as per IS 875-Part 2 (1987), live load and floor finish load have been considered as 5 kN/m² and 1 kN/m², respectively. The preliminary dimensions of beams and columns have chosen using the minimum dimensions clause given in ductile detailing code (IS 13920: 2016) and serviceability criteria recommended in IS 456 (2000). Intermediate building frame, subjected to 4 m full tributary loading, has designed using the limit state design approach.

The column size (450 mm × 450 mm) and beam size (300 mm × 450 mm) have been kept constant for all bare frames and all floors. However, for the irregular mass floor, the beam size is different as per the design requirement. It has verified that the sum of column design strength will be 1.4 times greater than the sum of beam design strength at any beam-column joint.

Time history analysis

To get to know the seismic behavior, elastic and inelastic response of buildings investigated from time history analysis. Dynamic analysis of linear and nonlinear models carried

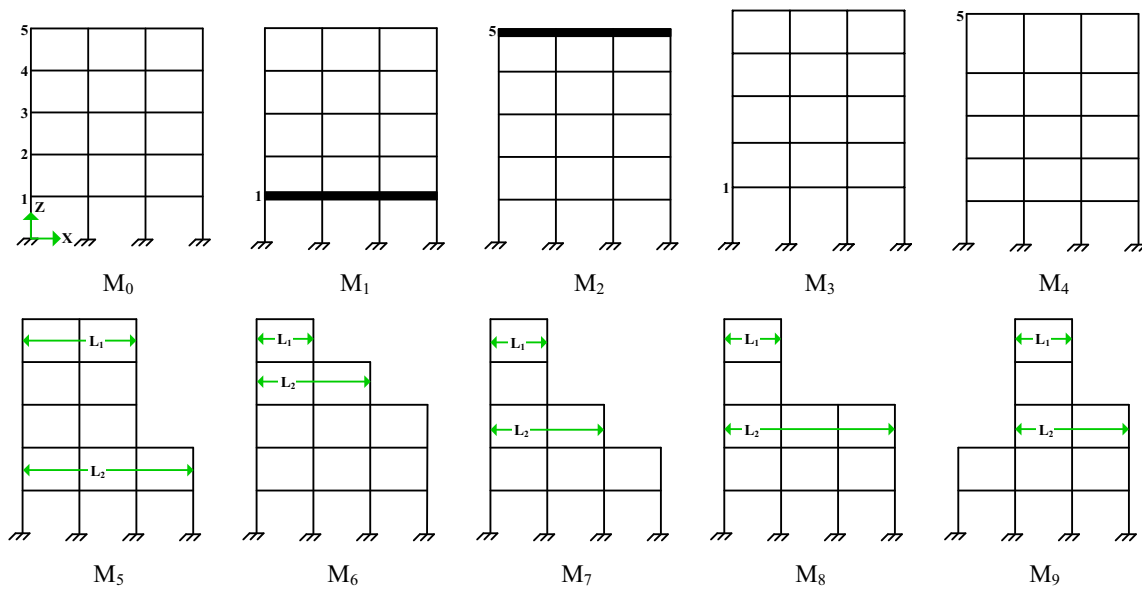


Fig. 1 Elevation of 5 storey RC moment resisting building frames

Table 1 Vertical geometric irregularity ratio

	M_5	M_6	M_7	M_8	M_9
L_2/L_1 (refer Fig. 1)	1.5	2	2	3	2

out using SAP2000 (Structural Analysis Program) CSI, version 21 (2018). In linear modeling, beam-column modeled as an elastic element with the gross moment of inertia. In the nonlinear analysis, Takeda hysteretic behavior (Takeda et al. 1970) has used for pretending the degradation of the RC element. As per ASCE 41-17 (2017), the nonlinear behavior of RC members, simulated by lumped plastic hinges at both ends of the member. The actual geometry of buildings with designed steel reinforcement has defined to determine the moment–curvature diagram. The selection procedure of ground motion used in the current study described in the subsequent section.

Selection and scaling of ground motion records

The artificial or simulated accelerograms, which can be generated from computer-aided programs and then modified iteratively to matches with the target response spectra (Bommer and Acevedo 2004). Some studies (Iervolino and Cornell 2005; Baker 2007; Iervolino et al. 2008; Araújo et al. 2016) emphasized that the use of artificial or simulated accelerograms produced an unrealistic and scattered response. While now a days, real ground-motion records easily accessible from Pacific Earthquake Engineering Research Center (PEER) (2005) NGA-West2 Database. As a result,

many researchers (Bhatt and Bento 2012; Bagheri et al. 2013; Senaldi et al. 2014) encouraging its usage in response assessment. Several national standards such as American Standard (ASCE-7), Eurocode 8 (EC8-1), and New Zealand Standard (NZS 1170.5: 2004) permit the use of real ground-motion records, and the guidelines are available for their selection. Hence, in this study, according to ASCE 7-16 (2016), 11 pairs of orthogonal horizontal ground motion components (Table 2) have been selected to acquire mean response as recommended by Bommer and Acevedo (2004). As per FEMA P695 (2009), in record sets, maximum two records from one event chosen to sidestep event-based bias.

The classification of soil in IS 1893-Part 1 (2016) has given by soil type and SPT value (Standard Penetration Test). In comparison, other national standards site classification provided in terms of average seismic shear velocity (V_{S30}). In this study, the building has considered on medium soil, which is corresponding to site class D of ASCE 7 ($180 < V_{S30} < 360$ m/s) as per Adhikary and Singh (2012). Amplitude scaling incorporated as per the ASCE 7-16 (2016) clauses, which recommend that the average spectra of the ground motions shall not drop below 90% of the target response spectrum within the code specified period range. The upper limit of this period range is 2.0 times the largest first mode period, and the lower limit is the period range consists of at least the number of modes essential to accomplish 90% mass participation in the principal horizontal direction. Table 3 and Fig. 2 illustrated the first three modal period and linear mode shapes. Table 4 shows the mass participation ratio of the 12 modes of the considered building. As proposed by Araújo et al. (2016), Kumbhar

Table 2 Details of selected ground motions for time history analysis

Record Sequence Number	Earthquake name	Year	Station name	Magnitude	Rjb (km)	Vs30 (m/s)
169	Imperial Valley-06	1979	Delta	6.53	22.03	242.05
728	Superstition Hills-02	1987	Westmorland Fire Sta	6.54	13.03	193.67
730	Spitak_Armenia	1988	Gukasian	6.77	23.99	343.53
777	Loma Prieta	1989	Hollister City Hall	6.93	27.33	198.33
960	Northridge-01	1994	Canyon Country—W Lost Cany	6.69	11.39	325.6
1116	Kobe_Japan	1995	Shin-Osaka	6.9	19.14	256
4883	Chuetsu-oki_Japan	2007	Niigata Nishi Kaba District	6.8	27.83	254.68
5774	Iwate_Japan	2008	Nakashinden Town	6.9	29.37	276.3
6953	Darfield_New Zealand	2010	Pages Road Pumping Station	7	24.55	206
6969	Darfield_New Zealand	2010	Styx Mill Transfer Station	7	20.86	247.5
8134	Christchurch_New Zealand	2011	Styx Mill Transfer Station	6.2	11.24	247.5

Table 3 Modal time period (seconds) of the considered building models

	M_0	M_1	M_2	M_3	M_4	M_5	M_6	M_7	M_8	M_9
Mode 1	0.74	0.72	0.86	0.89	0.77	0.66	0.61	0.56	0.57	0.56
Mode 2	0.23	0.24	0.25	0.27	0.29	0.24	0.22	0.24	0.25	0.24
Mode 3	0.13	0.14	0.13	0.14	0.15	0.13	0.13	0.13	0.13	0.13

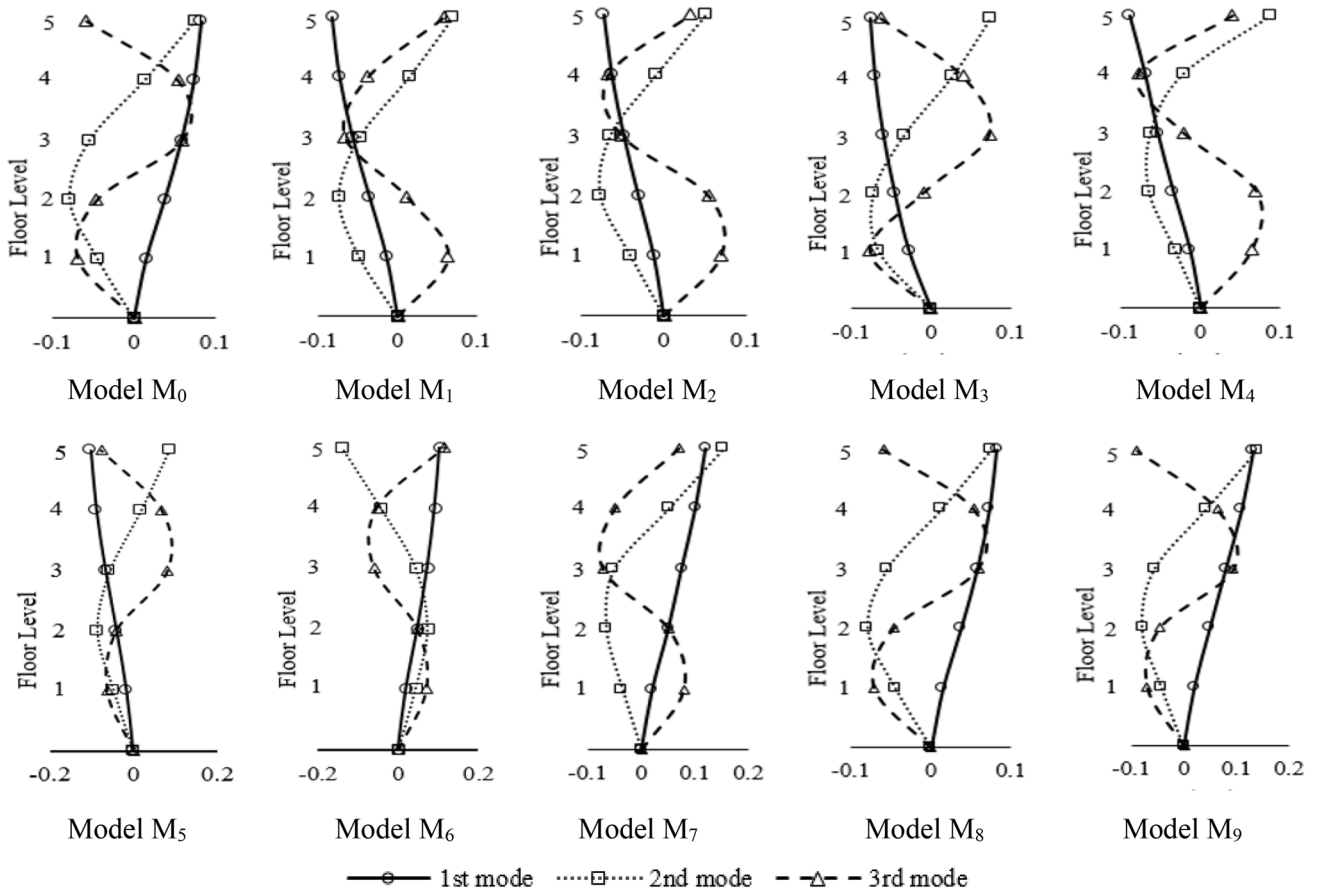


Fig. 2 Linear mode shape for considered building models

Table 4 Modal mass participation ratio of the considered building models

	M_0		M_1		M_2		M_3		M_4		M_5		M_6		M_7		M_8		M_9	
	UX	UZ	UX	UZ	UX	UZ	UX	UZ	UX	UZ	UX	UZ	UX	UZ	UX	UZ	UX	UZ	UX	UZ
Mode 1	0.82	0	0.75	0	0.83	0	0.91	0	0.80	0	0.76	0	0.81	0	0.73	0	0.78	0	0.73	0
Mode 2	0.93	0	0.92	0	0.94	0	0.98	0	0.91	0	0.92	0	0.91	0	0.90	0	0.90	0	0.90	0
Mode 3	0.97	0	0.99	0	0.98	0	1	0	0.96	0	0.96	0	0.97	0	0.96	0	0.97	0	0.96	0
Mode 4	0.99	0	1	0	1	0	1	0	0.99	0	1	0	0.99	0	1	0	0.99	0	1.00	0
Mode 5	1	0.64	1	0.62	1	0.64	1	0.68	1	0.63	1	0.21	1	0	1	0	1	0	1	0
Mode 6	1	0.64	1	0.62	1	0.64	1	0.68	1	0.63	1	0.48	1	0.45	1	0.48	1	0.45	1	0.56
Mode 7	1	0.64	1	0.62	1	0.64	1	0.68	1	0.63	1	0.63	1	0.49	1	0.59	1	0.55	1	0.66
Mode 8	1	0.88	1	0.85	1	0.88	1	0.92	1	0.87	1	0.80	1	0.78	1	0.81	1	0.78	1	0.80
Mode 9	1	0.88	1	0.85	1	0.88	1	0.92	1	0.87	1	0.84	1	0.89	1	0.90	1	0.90	1	0.90
Mode 10	1	0.94	1	0.94	1	0.94	1	0.96	1	0.93	1	0.92	1	0.93	1	0.94	1	0.93	1	0.96
Mode 11	1	0.94	1	0.94	1	0.94	1	0.96	1	0.93	1	0.95	1	0.95	1	0.96	1	0.95	1	0.96
Mode 12	1	0.97	1	0.98	1	0.97	1	0.98	1	0.96	1	0.97	1	0.97	1	0.98	1	0.97	1	0.97

and Kumar (2020), a supplementary condition of imposing spectral mismatch limits relative to target spectrum (IS 1893-Part 1: 2016), have been employed $\pm 50\%$, to diminish the record-to-record unevenness. Figure 3 shows that the mean spectra of the individual ground motion spectra, which is well above the 90% of target spectra.

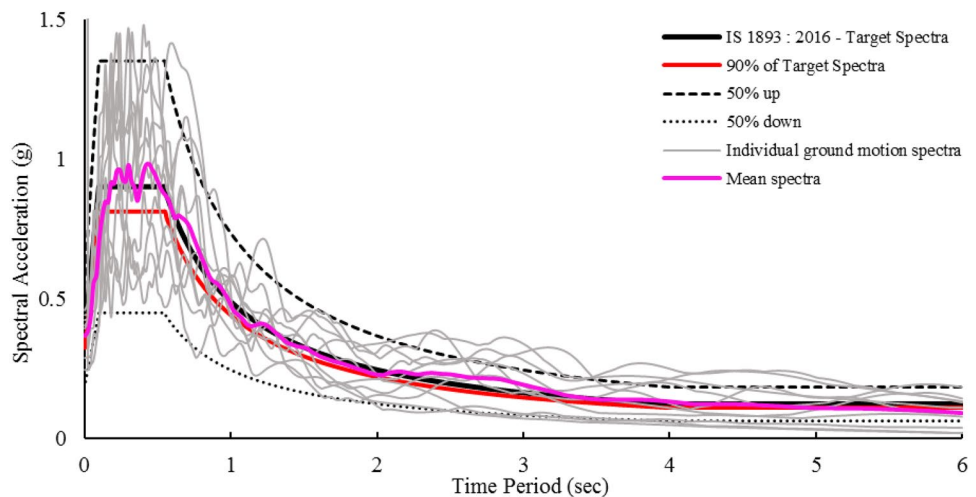
Results and discussion

Elastic and inelastic FRS

Time history analysis of 10 buildings, under 11 earthquake records are executed individually on elastic and inelastic models. The ‘X’ direction acceleration time histories, at various floor levels, are recorded for each ground motion to get FRS. These FRS obtained with a 5% damping ratio and a mean results are plotted (spectral acceleration ‘Sa’ in

‘g’ unit on the vertical axis and time period ‘T’ in seconds on the horizontal axis), in Fig. 4, for each floor. These spectra give the acceleration demand on NSC, which is attached to the level. Figure 4 displays the elastic FRS with a dotted line and inelastic FRS with solid lines for all the five-story regular and irregular building frames (M_0 – M_9). Figure 4 shows there is a sequential increase in response from the lower first floor to the upper fifth floors (Shooshtari et al. 2010). Also, FRS is indicating the distinct peaks analogous to contributing modes due to the dynamic characteristics of the building (Kumar et al. 2011). As mentioned by Petrone et al. 2015, because of the dynamic filtering effect, the floor accelerogram intensified with respect to the base and has an enormous frequency content for the time periods, near to the vibration time periods of the elastic model. Similar outcomes have observed in the present study considered buildings. The peaks are recorded very nearer to these elastic modal time

Fig. 3 Individual response spectra of the 11-ground motion record set, its mean spectra and IS 1893(1):2016 Target spectra of zone V (PGA=0.36 g) for medium soil



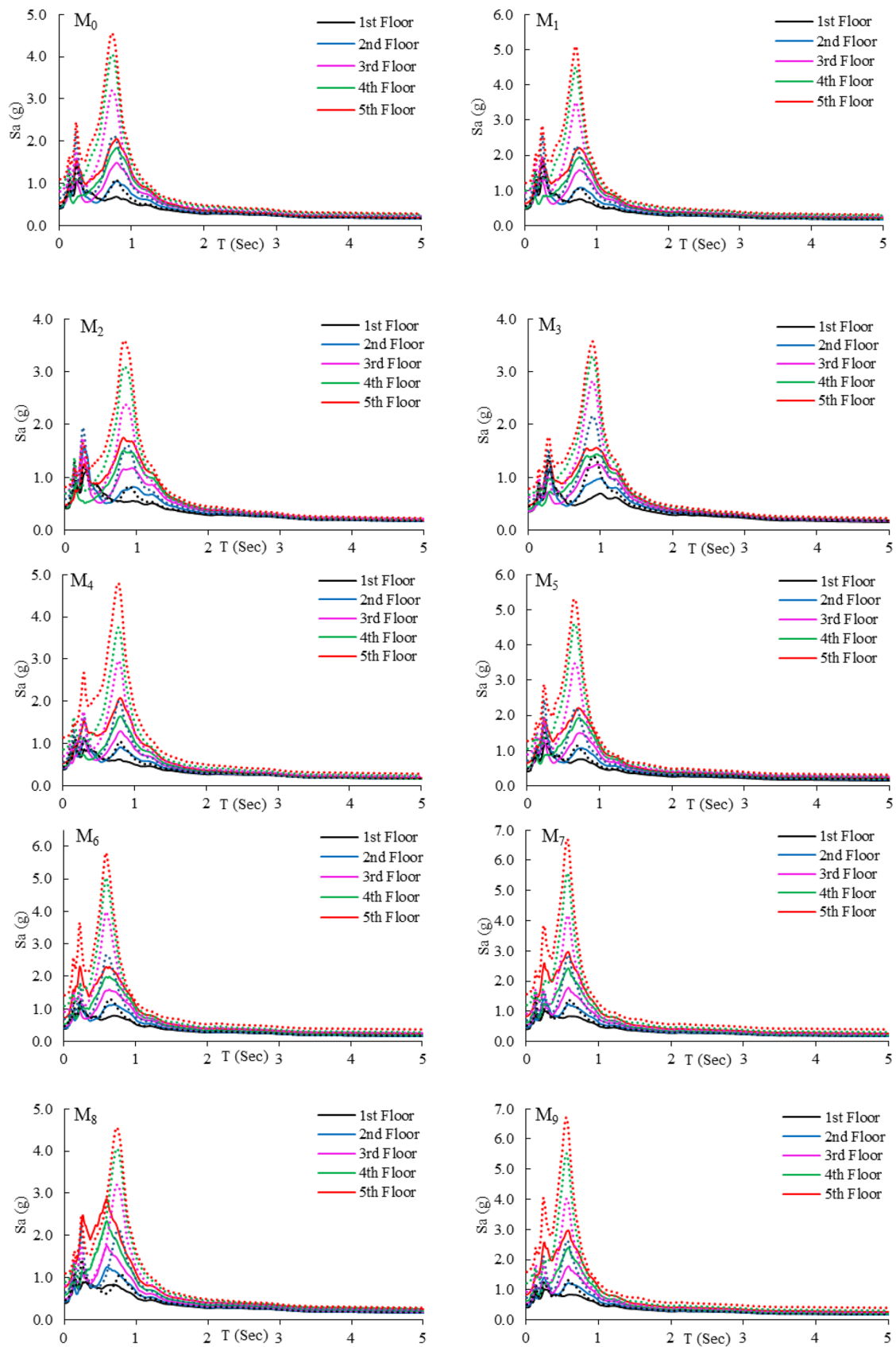


Fig. 4 Elastic (dotted line) and inelastic (solid line) FRS of 5-storey considered buildings

periods (Table 3). It has also noted at first sight that, in inelastic FRS (solid lines) considerable reduction in floor spectral accelerations as compared to elastic FRS (Chaudhuri and Villaverde 2008; Weiser et al. 2013; Flores et al. 2015).

For better and more proper understanding, floor to floor comparison of irregular buildings (M_1 – M_9) with the regular building (M_0) has also done. The first floor and the fifth floor relative graphs for elastic and inelastic models are shown in Figs. 5 and 6, respectively. 1st peak, 2nd peak, and 3rd peak

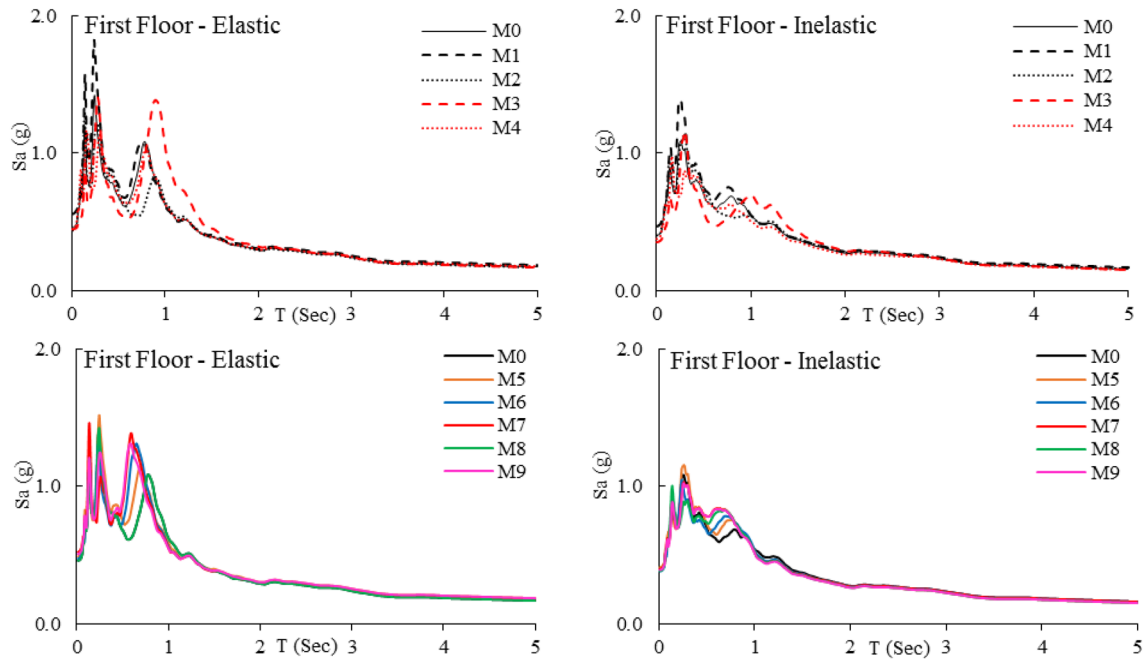


Fig. 5 First floor elastic and inelastic FRS of 5-storey considered buildings

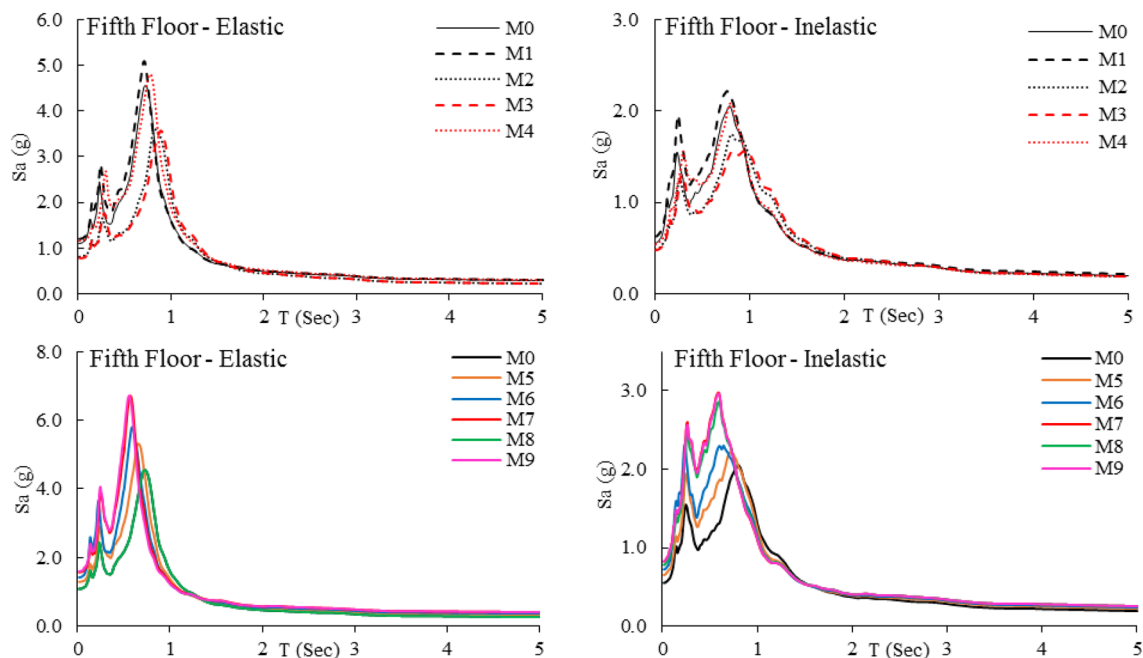


Fig. 6 Fifth floor elastic and inelastic FRS of 5-storey considered buildings

has specified as the maximum spectral acceleration very close or nearer to the 1st, 2nd, and 3rd mode time period, respectively. For lower storey elastic models (Fig. 5), three peaks observed, in which 2nd and 3rd peak acceleration values are foremost and M_1 model is giving a maximum response. In lower storey inelastic models (Fig. 5), 2nd peak is foremost, and here also, the M_1 model, i.e., mass irregularity present at the first story, is giving a maximum response. Also, the response governed by input ground motion characteristics as the shape of the FRS follows the input ground motion spectra (Kumar et al. 2011). For higher storey elastic models (Fig. 6), 1st peak spectral acceleration values are uppermost in elastic models, and for inelastic models, 1st and 2nd peak are observed but 1st peak spectral acceleration values are highest.

Floor amplification evaluation

The ratio between the peak floor spectral acceleration (PFSa) and peak ground acceleration (PGA) directed against the relative height in Fig. 7. The response is normalized, i.e., maximum over the complete spectrum, in directive to study

the floor acceleration magnification of irregular building, with respect to height. The elastic building models, which is representing the average response of 11 ground motions, displays a nearly linear tendency (Petrono et al. 2015). The value of the ratio PFSa/PGA for M_0 reaches close to 4.3 on the fifth floor. At a similar relative height, the value of the ratio PFSa/PGA for mass irregularity present at the first story, i.e., M_1 model, is higher. Also for the vertical geometric irregular buildings, the value of the ratio PFSa/PGA, for all the relative heights is larger than M_0 and M_1 .

The inelastic model also exhibits a closely linear tendency with a smaller amplification. When the stiffness irregularity is present at the lower story (i.e., M_3 model), amplification is higher than the regular model only in the lower story. Also, when the mass and stiffness irregularity is present at the higher story (i.e., M_2 ; M_4 model), amplification is smaller than the regular building model. In geometric irregular buildings (i.e., M_5 – M_9 model), it also observed that at the top floor level with a significantly reduced mass than the mass of the typical floor, amplification is more significant (Surana et al. 2018). This large amplification is because of the tuning of the top story to the rest of the building storey.

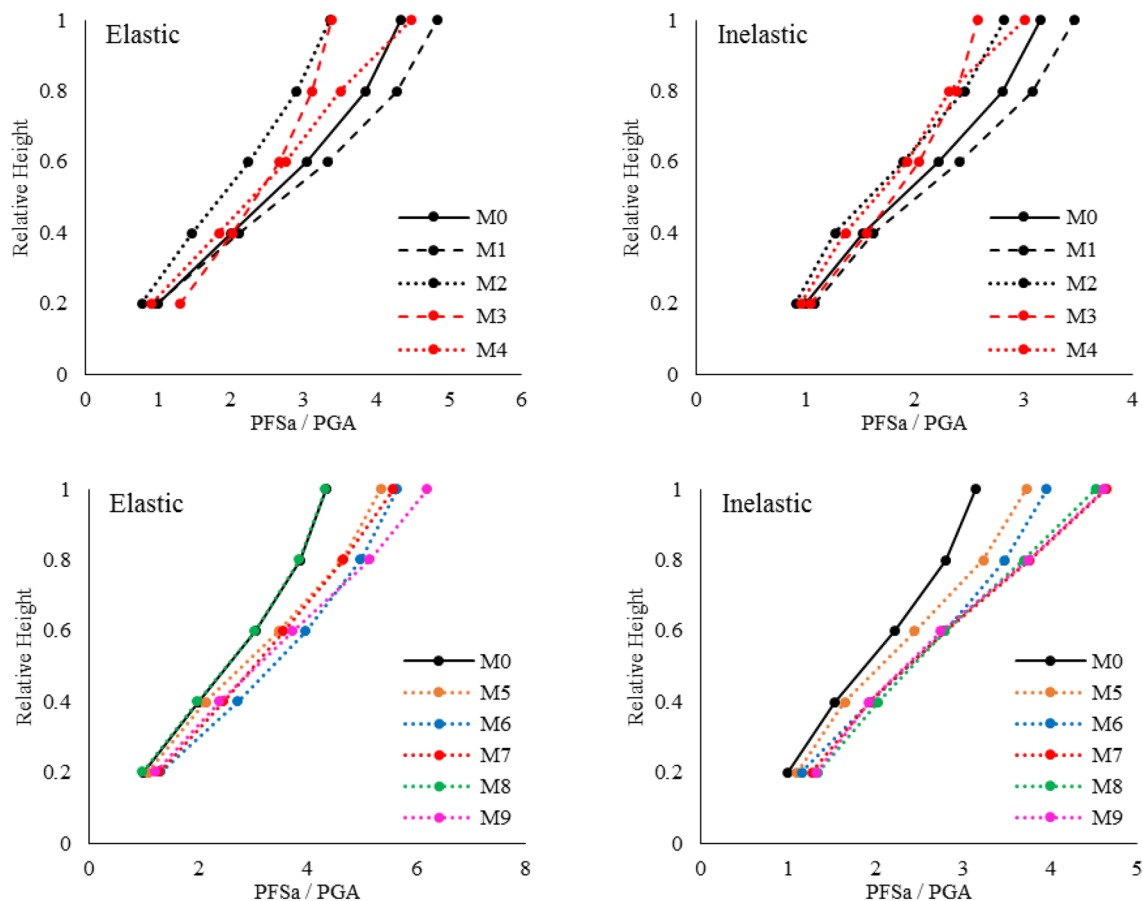


Fig. 7 Normalized floor amplification of elastic and inelastic 5-storey building models

Conclusion

Analytical study of regular and irregular building models subjected to 11 number of ground motions has carried out in the present study. The primary intension of this study is to recognize and quantify increase in the floor acceleration of the low rise building models, which is the most significant parameter affecting the design of non-structural components. From the study, important research outcomes as follows.

- i. Even if the elastic and inelastic models display a nearly linear tendency in floor amplification, the structural nonlinearity results in decreases in the floor response spectra. They are signifying that structural inelasticity has a beneficial effect on non-structural components design acceleration demand.
- ii. The occurrence of mass irregularity at lower storey and the presence of geometric irregularity in buildings amplified the floor acceleration response.
- iii. In most of the industrial buildings, these irregularities will act altogether, which may further amplified the response indicating the structural designer's role to be more vigilant during the design of the non-structural components support system.

Compliance with ethical standards

Conflict of interest On behalf of all authors, the corresponding author states that there is no conflict of interest.

References

- Adam, C. (2001). Dynamics of elastic-plastic shear frames with secondary structures: Shake table and numerical studies. *Earthquake Engineering and Structural Dynamics*. [https://doi.org/10.1002/1096-9845\(200102\)30:2<257:AID-EQE7>3.0.CO;2-J](https://doi.org/10.1002/1096-9845(200102)30:2<257:AID-EQE7>3.0.CO;2-J).
- Adhikary, S., & Singh, Y. (2012). Limitations of soil amplification provisions in the 2002 Indian seismic code. *Journal of Earthquake Engineering*. <https://doi.org/10.1080/13632469.2011.594485>.
- Agarwal, A. K., & Datta, T. K. (2003). Response of multiple-supported secondary system on torsionally coupled yielding primary system. *Advances in Vibration Engineering*, 2(4), 115–124.
- Amin, M., Hall, W. J., Newmark, N. M., & Kassawara, R. P. (1971). Earthquake response of multiply connected light secondary systems by spectrum methods. In: *Proceedings of the 1st national conference on pressure vessels and piping*, New York, pp. 103–29.
- Araújo, M., Macedo, L., Marques, M., & Castro, J. M. (2016). Code-based record selection methods for seismic performance assessment of buildings. *Earthquake Engineering & Structural Dynamics*. <https://doi.org/10.1002/eqe.2620>.
- ASCE/SEI 41-17. (2017). *Seismic evaluation and retrofit of existing buildings*. Reston: American Society of Civil Engineers.
- ASCE/SEI 7-16. (2016). *Minimum design loads and associated criteria for buildings and other structures*. Reston: American Society of Civil Engineers.
- Bagheri, B., Nivedita, A. K., & Firoozabad, E. S. (2013). Comparative damage assessment of irregular building based on static and dynamic analysis. *International Journal of Civil & Structural Engineering*, 3(3), 505–512.
- Baker, J. W. (2007). Measuring bias in structural response caused by ground motion scaling. In: *CD ROM proceedings of the 8th Pacific conference on earthquake engineering, Singapore*. Paper no. 56.
- Bhatt, C., & Bento, R. (2012). Comparison of nonlinear static methods for the seismic assessment of plan irregular frame buildings with non-seismic details. *Journal of Earthquake Engineering*. <https://doi.org/10.1080/13632469.2011.586085>.
- Biggs, J. M., & Roesset, J. M. (1970). Seismic analysis of equipment mounted on a massive structure. *Seismic design of nuclear power plants*. New York: MIT press.
- Bommer, J. J., & Acevedo, A. B. (2004). The use of real earthquake accelerogram as input to dynamic analysis. *Journal of Earthquake Engineering*, 8(1), 43–91.
- Chaudhuri, S. R., & Villaverde, R. (2008). Effect of building nonlinearity on seismic response of non-structural components: A parametric study. *Journal of Structural Engineering*, 134(4), 661–670.
- Chen, Y., & Soong, T. T. (1988). State-of-the-art-review: Seismic response of secondary systems. *Engineering Structures*, 10(4), 218–228.
- CSI, version 21. (2018). *Integrated finite element analysis and design of structures basic analysis reference manual*. Berkeley: Computers and Structures Inc.
- FEMA P695. (2009). *Quantification of building seismic performance factors*. Washington, DC: Federal Emergency Management Agency.
- Flores, F. X., Garcia, D. L., & Charney, F. A. (2015). Assessment of floor accelerations in special steel moment frames. *Journal of Constructional Steel Research*, 106, 154–165.
- HAZUS. (2006). HAZUS-MH MR1/MR2, Technical Manual, developed by the Federal Emergency Management Agency through agreements with the National Institute of Building Sciences, Washington, D.C.
- IS 13920. (2016). *Ductile design and detailing of reinforced concrete structures subjected to seismic forces—code of practice (first revision)*. New Delhi: Bureau of Indian Standards.
- IS 1893-Part 1. (2016). *Criteria for earthquake resistant design of structures. Part 1 general provision and buildings*. New Delhi: Bureau of Indian Standards.
- IS 456. (2000). *Plain and reinforced concrete—code of practice (fourth revision)*. New Delhi: Bureau of Indian Standards.
- IS 875-Part 1. (1987). *Code of practice for design loads (other than earthquake) for buildings and structures: part 1-dead loads (second revision)*. New Delhi: Bureau of Indian Standards.
- IS 875-Part 2. (1987). *Code of practice for design loads (other than earthquake) for buildings and structures: part 2—Imposed Loads (second revision)*. New Delhi: Bureau of Indian Standards.
- Kumar, R., Singh, Y., & Tripathi, S. (2011). Effect of building performance on floor response spectra. *Journal of Structural Engineering (Madras)*, 37(6), 422–426.
- Kumbhara, O. G., & Kumar, R. (2020). Performance assessment of RC frame designed using force, displacement & energy-based approach. *Structural Engineering and Mechanics*, 73(6), 699–714.
- Medina, R. A., Sankaranarayanan, R., & Kingston, K. M. (2006). Floor response spectra for light components mounted on regular moment-resisting frame structures. *Engineering Structures*, 28(14), 1927–1940.

- Menon, A., & Magenes, G. (2011). Definition of seismic input for out-of-plane response of masonry walls: II. formulation. *Journal of Earthquake Engineering*, 15(2), 195–213.
- Pacific Earthquake Engineering Research Center. (2005). PEER Ground Motion <https://ngawest2.berkeley.edu/>. Accessed 28 Mar 2020
- Petrone, C., Magliulo, G., & Manfredi, G. (2015). Floor response spectra in RC frame structures designed according to Eurocode 8. *Article in Bulletin of Earthquake Engineering*, 14(3), 747–767.
- USNRC Regulatory Guide 1.122. (1978). *Development of floor design response spectra for seismic design of floor-supported equipment or components*, Rev. 1.
- Rodriguez, M. E., Restrepo, J. I., & Carr, A. J. (2002). Earthquake-induced floor horizontal accelerations in buildings. *Earthquake Engineering and Structural Dynamics*, 31(3), 693–718.
- Sankaranarayanan, R., & Medina, R. A. (2007). Acceleration response modification factors for nonstructural components attached to inelastic moment-resisting frame structures. *Earthquake Engineering and Structural Dynamics*, 36(14), 2189–2210.
- Senaldi, I., Magenes, G., Penna, A., Galasco, A., & Rota, M. (2014). The effect of stiffened floor and roof diaphragms on the experimental seismic response of a full-scale unreinforced stone masonry building. *Journal of Earthquake Engineering*. <https://doi.org/10.1080/13632469.2013.876946>.
- Shooshtari, M., Saaticioglu, M., Naumoski, N., & Foo, S. (2010). Floor response spectra for seismic design of operational and functional components of concrete buildings in Canada. *Canadian Journal of Civil Engineering*, 37(12), 1590–1599.
- Singh, A. K., & Ang, A. H. (1974). Stochastic prediction of maximum seismic response of light secondary systems. *Nuclear Engineering and Design*, 29(2), 218–230.
- Singh, M. P., Moreschi, L. M., Suarez, L. E., & Matheu, E. E. (2006a). Seismic design forces I: Rigid non-structural components. *Journal of Structural Engineering*, 132(10), 1524–1532.
- Singh, M. P., Moreschi, L. M., Suarez, L. E., & Matheu, E. E. (2006b). Seismic design forces I: Flexible non-structural components. *Journal of Structural Engineering*, 132(10), 1533–1543.
- Soong, T. T. (1994). Seismic behavior of nonstructural elements state-of-the-art report. In: *Proceedings, 10th European conference on earthquake engineering*.
- Suarez, L. E., & Singh, M. P. (1987). Floor response spectra with structure–equipment interaction effects by a mode synthesis approach. *Earthquake Engineering & Structural Dynamics*, 15(2), 141–158.
- Surana, M., Singh, Y., & Lang, D. H. (2018). Floor spectra of inelastic RC frame buildings considering ground motion characteristics. *Journal of Earthquake Engineering*. <https://doi.org/10.1080/13632469.2016.1244134>.
- Takeda, T., Sozen, M. A., & Nielsen, N. N. (1970). Reinforced concrete response to simulated earthquakes. *Journal of the Structural Division*, 96(12), 2557–2573.
- Villaverde, R. (1997). Seismic design of secondary structures: State of the art. *Journal of Structural Engineering*, 123(8), 1011–1019.
- Villaverde, R. (2004). Seismic analysis and design of non-structural elements. *Earthquake engineering* (pp. 1156–1220). Boca Raton: CRC Press.
- Wieser, J., Pekcan, G., Zaghi, A. E., Itani, A., & Maragakis, M. (2013). Floor accelerations in yielding special moment resisting frame structures. *Earthquake Spectra*, 29(3), 987–1002.

Publisher's Note Springer Nature remains neutral with regard to jurisdictional claims in published maps and institutional affiliations.